INVESTIGATION OF STRUCTURAL AND ELECTRICAL PROPERTIES OF Ce^{3+} IONS SUBSTITUTED Cd-Co FERRITES

K. HUSSAIN[a], N. AMIN[a], M. AJAZ-UN-NABI[a]. A. ALI[a], K. MAHMOOD[a], G. MUSTAFA[b], M. SHARIF[a], M. S. HASAN[c], N. SABIR[a], S. ALI[a], F. JABEEN[d], M. ASIF[e], M. I. ARSHAD[a,*]

[a]*Department of Physics, Government College University, Faisalabad 38000, Pakistan*

[b]*Department of Physics, Bahauddin, Zakariya University Multan, 60800, Pakistan*

[c]*Department of Physics, The University of Lahore, 1-kM Raiwind Road, Lahore, Pakistan*

[d]*Cardiovascular and Metabolic Research Unit, Laurentian University, 935 Ramsey Lake Road, Sudbury, ON, Canada*

[e]*Department of Physics, COMSATS University, Islamabad, Lahore Campus,54500 Lahore, Pakistan*

In this work we study the structural and electrical properties of Ce^{3+}-substituted cadmium cobalt ferrites having composition $Cd_{0.35}Co_{0.65}Fe_{2-x}Ce_xO_4$ with x = 0.00, 0.01, 0.02, 0.03, 0.04 and 0.05, which were prepared by co-precipitation method. The structural properties have been investigated with XRD and FTIR techniques. The IV characteristics have also been studied of Ce^{3+} substituted nano-particles. The XRD patterns confirm the growth of single phase spinel structure of our samples. The crystallite size calculated from XRD results was in the range of 21.6 – 34.7 nm. The lattice parameter was found in the range of 8.47 - 8.67Å. The Current-Voltage characteristics show that resistivity of samples decreases with increasing temperature which confirms their semiconductor nature. The IR studies confirm the structure of the synthesized samples. The absorption bands observed around 442 cm^{-1} and 546 cm^{-1} are associated with the tetrahedral (A-site) and octahedral (B-site) stretching vibrations. The elemental compositions measured from EDX are in close agreement with the expected stoichiometric ratios of the reactant solutions. It is also explored that electrical resistivity increases with the increase of cerium substitution and it is in the range of 1.584×10^7 - 42.83×10^7 Ω-cm. In UV-Vis spectra, the observed peak indicates that nanocomposites are photoactive compounds and their potential to use in optoelectronic applications. These nanoparticles also have applications in magnetic recording media, security switching and high frequency applications.

(Received September 5, 2018; Accepted January 23, 2019)

Keywords: Spinel ferrites, Co-precipitation, XRD, DC-Resistivity

1. Introduction

The spinel ferrites have become an interesting subject for researchers due to their exclusive properties like high coercivity, good stability, moderate saturation magnetization, mechanical hardness, optical, magneto properties and low electric losses [1-2]. Due to semiconductor nature, ferrites have great attraction and wide range of applications in clinical and technological areas such as in making of transformers, inductor coils, chokes, magneto optical displays, permanent magnets, gas sensors, antenna rods, biomedicine, and magnetic resonance imaging [3-5]. As significant parts of magnetic materials, the use of ferrites on large scale are in electronic industry, mining, oil energy industry, medical treatment, industrial automation, metallurgy, components of computers, storage devices, microwave application, recording media, hyperthermia for cancer, refrigeration, magnetic resonance imaging and civil industry because of

*Corresponding author: miarshadgcuf@gmail.com

their high coercive force, high electric resistance, economical cost and longtime stability [6-10]. In microwave appliances, ferrites are used due to small eddy current losses [11]. Spinel ferrite nanoparticles are chemically and thermally stable nanocomposites with general formula, AB_2O_4, where A shows the divalent ions (Co^{2+}, Zn^{2+}, Fe^{2+}, Mg^{2+}, Ni^{2+}, Cd^{2+}) [12]. Many research studies have been found in the literature depicting the semiconducting nature of nano ferrites [13]. Various methods have been reported to prepare the spinel ferrites such as hydrothermal, sol-gel combustion, micro emulsion method etc. Among these, co-precipitation method has attained much attention of the researchers due to greater reactivity and high homogeneity in particle size [14]. Many studies also have been found reporting the alteration of structural and electrical properties of spinel ferrites using the substitution of rare earth metals [15-17]. In present research work, Ce-substituted Cd-Co ferrites with composition $Cd_{0.35}Co_{0.65}Fe_{2-x}Ce_xO_4$ spinel ferrites has been chosen to investigate the effect of Ce doping on the structural and electrical characteristics as rare earth ions when placed into the spinel structure causes structural distortion. The electrical transport properties of materials highly depend upon crystal structure, so this distortion can be used to control the electrical properties of spinel ferrites. There are many reports of the substitution of rare earth elements (Tb, Dy, Yb, Er, Gd, Sm, Ce, Y, Eu, La, Th, etc.), in spinel ferrites [8-12].

2. Materials and method

2.1. Sample preparation

In this study, ferrite nano particles with composition $Cd_{0.35}Co_{0.65}Fe_{2-x}Ce_xO_4$ (x= 0.00, 0.01, 0.02, 0.03, 0.04 and 0.05) were prepared using co-precipitation method. The main objective was to examine effect of Ce^{3+} cations on the structural and electrical properties of ferrites. The highly purred salts $FeCl_3.6H_2O$, $CdCl_3.2.5H_2O$, $CoCl_3.6H_2O$, $CeCl_3.7H_2O$, and NaOH were used to obtain the nano particles with required composition. The above mentioned salts were taken according to the stoichiometric ratios and mixed in DI water to obtain aqueous solutions. These solutions were then mixed using magnetic stirrer with hot plate at temperature 60 ^oC. During stirring process, NaOH was added drop wise to maintain the pH at 11-12. Then precipitates were washed several times with double distilled water to eliminate the unwanted salt and other impurities. Thereafter precipitates were dried in an oven at 100 °C. The dried precipitates were then sintered at 950 ^oC for 6 hours. The annealed samples were grinded to obtain fine powder of nano ferrites. The spinel structure of the samples was verified using X-ray diffractometer (Xpert Pro PANalytical diffractometer) with $Cu_{K\alpha}$ source having wavelength 0.154 nm. The elemental analysis was done using EDX. The Fourier transform infrared (FTIR) spectra were recorded in the range 400 – 4000 cm^{-1} using Jasco-310 spectrometer. The powdered samples were pressed into disk shaped pallets and I-V data was obtained using two probe method to analyze the electrical nature of the samples.

2.2. Calculation

The structural parameters like lattice constant ‘a’, unit cell volume, X-ray density and crystallite size were calculated from XRD data using these equations as under below [18-21].

$$a = \frac{\lambda}{2Sin\theta}\sqrt{h^2 + k^2 + l^2} \quad (1)$$

$$V_{cell} = a^3 \quad (2)$$

$$Dx = \frac{ZM}{N_A\, a^3} \quad (3)$$

$$D = \frac{k\lambda}{\beta_{hkl}\, Cos\theta} \quad (4)$$

Here (h k l) are the Miller indices, V_{cell} is the unit cell volume, Z is representing 8 molecules per unit cell of the spinel structure, N_A is the Avogadro’s number, M is the molecular

weight of the sample, where k is the shape factor, λ is the X-ray wavelength; θ is the Bragg's diffraction angle and β_{hkl} represents full width at half maxima.

3. Results and discussion

3.1. X-ray diffraction analysis

Fig 1 shows the XRD patterns of synthesized samples that confirm the single phase spinel structure of $Cd_{0.35}Co_{0.65}Fe_{2-x}Ce_xO_4$ (JCPDS No. 9009923). The obtain patterns have diffraction peaks with reflection planes of (220), (311), (222) (400), (422) and (333) which is indexed by computer software. The (311) is the sharpest peak in all XRD patterns. The crystallite size of each sample was measured using Scherer Eq.4 where β is the line broadening at FWHM in radians, θ is Bragg angle and X-ray wavelength is λ=1.542Å.

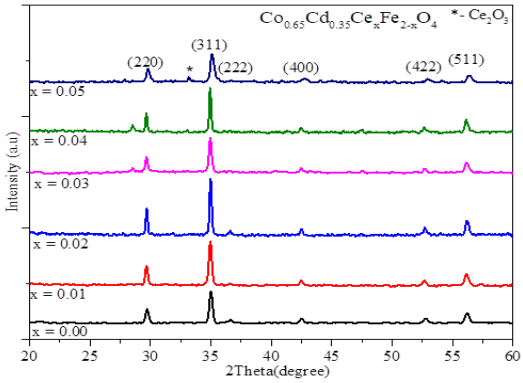

Fig. 1. XRD Patterns of $Cd_{0.35}Co_{0.65}Fe_{2-x}Ce_xO_4$ *(0.00 ≤ x ≤ 0.05).*

The determined physical parameters from the XRD data are presented in Table 1. The calculated crystallite size and lattice constant are found in the range 21.6 - 34.7 nm and 8.47 Å -8.67 Å, respectively. The change in lattice constant is attributed to the ionic radii difference of Fe^{3+} (0.645 Å) and Ce^{3+} (1.143 Å) [22].

Table 1. Lattice constant, Unit cell volume (Å)^3, Crystallite size (nm) and Electrical Resistivity (Ω-cm) of $Co_{0.65}Cd_{0.35}Ce_xFe_{2-x}O_4$ *ferrites (0.00 ≤ x ≤ 0.05).*

Composition (x)	Lattice constant (Å)	Unit cell volume (Å)^3	Crystallite size (nm)	Resistivity (Ω-cm)×10^7
0	8.67	651.71	21.6	1.58
0.01	8.51	616.30	34.7	6.38
0.02	8.47	607.64	33.5	8.22
0.03	8.53	620.65	32.8	14.80
0.04	8.50	614.13	30.1	30.90
0.05	8.49	611.96	21.8	42.83

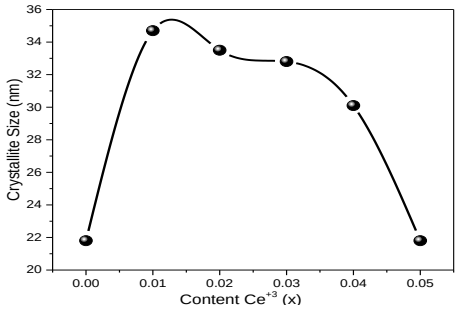

Fig. 2.Crystallite size (nm) vs. Ce content (x).

3.2. Energy dispersive X-ray analysis

Fig. 3 (a-b) shows the EDX spectra of the representative samples with x = 0.02 and 0.04. The elemental composition of the samples sintered at 950 °C is calculated from the EDX spectrum. The EDX spectra confirm the presence of each element Co, Cd, Ce, Fe and O in the samples and the proportion of these elements found to be in good agreement with the expected stoichiometric ratio [16]. It can be observed from the analysis of these spectra that a complete chemical reaction has occurred and all the undesired elements have been removed from the prepared samples.

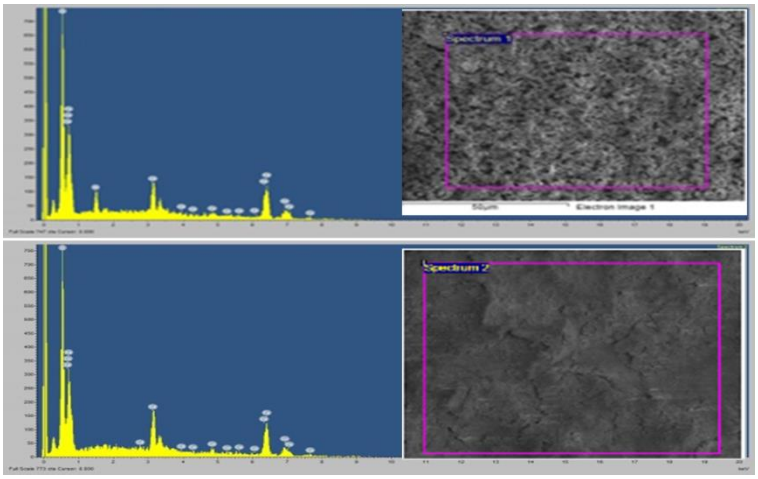

Fig. 3. EDX Spectrum for Ce^{3+}-substituted Cd-Co-ferrites at (a) x = 0.02 and (b) = 0.04.

3.3. FTIR analysis

FTIR spectra of synthesized $Co_{0.65}Cd_{0.35}Ce_xFe_{2-x}O_4$ ferrites are presented in Fig 4. The FTIR spectra have been recorded in the range of 400 - 4000 cm^{-1}. Two main absorption bands octahedral (υ_1) and tetrahedral (υ_2) that are the characteristic bands of spinel ferrites are observed around 442 cm^{-1} and 576 cm^{-1}, which confirm the formation of spinel ferrites [23].

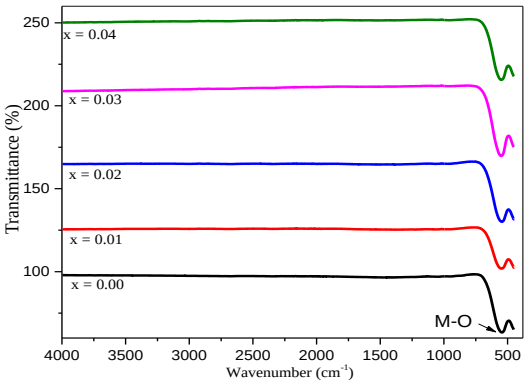

Fig. 4. FTIR Spectrum of $Co_{0.65}Cd_{0.35}Ce_xFe_{2-x}O_4$ ferrites ($0.00 \leq x \leq 0.04$).

3.4. Optical properties

High surface to volume ratio and reduced dimensionality of nano particles make them fascinating candidates for applications in optoelectronic devices. A large community of materials researchers is working to explore the field of nanoparticle to make them practically suitable for these applications. Optical bandgap is one of the major parameters to be controlled to use nanoparticles in the fabrication of devices. Fig. 5 represents absorption of light as a function of wavelength in the range of 200 -1100 nm. The sharpness in the peaks present in the UV-visible spectra confirms the formation of well spread colloids. An increasing trend in the absorption of light is observed with increase in Ce content [24]. The optical band gap of our samples was calculated using Tauc relation $\alpha h\upsilon = A(h\upsilon - E_g)^n$, where E_g is optical band gap, $h\upsilon$ is energy of incident photons, A is transition probability constant, α is absorption coefficient. The constant n is bandgap dependent constant and it exhibits a value of 0.5 for direct band gap materials and 2 for indirect bandgap materials [25-26]. These calculations are shown in Fig 6 & Fig 7 for n = 0.5 and n = 2, respectively.

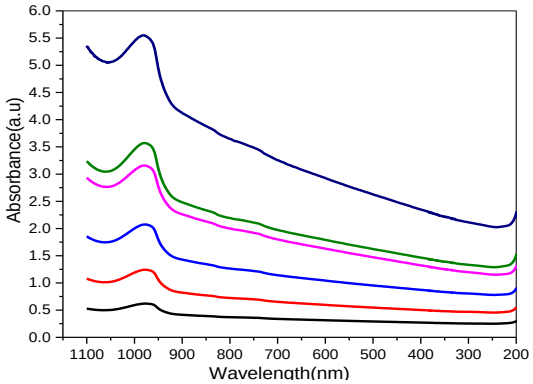

Fig. 5. Spectral absorbance of the Ce^{3+}-substituted Cd-Co ferrites ($0.00 \leq x \leq 0.05$).

The bandgap values calculated for n = 0.5 lies in the range 1.74 - 2.5 eV and the lowest bandgap value is observed at x = 0.04. Similarly, bandgap for n = 2 is observed in the range 3.5 – 4.5 eV. The similar behavior of spinel ferrites also has been reported in literature previously [16-17].

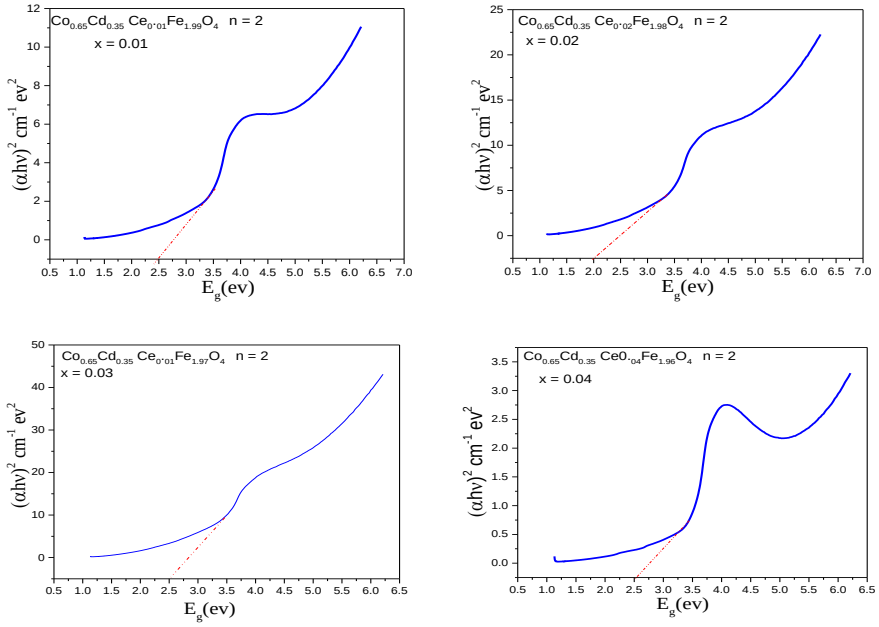

Fig. 6. Plot $(\alpha hv)^2$ versus $E_g(ev)$ (a) x = 0.01 (b) x = 0.02 (c) x = 0.03 and (d) x = 0.04.

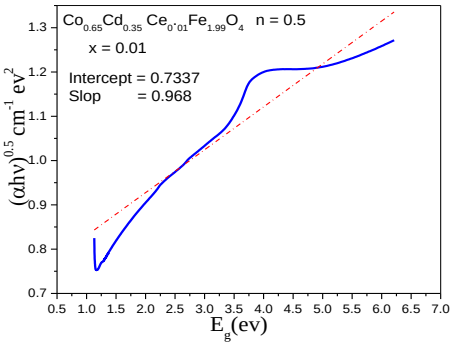

Fig. 7. Plot $(\alpha hv)^{0.5}$ versus $E_g(ev)$ where x = 0.01 and n = 2.

3.5. Variation of DC- resistivity with composition

Fig.8 (a) shows the variation in dc resistivity of spinel ferrites as a function of temperature. The resistivity values were calculated using the relation R = pL/A, where A is cross-sectional area of disk shaped samples, L is thickness of the samples and R is resistance of the pellet [27]. In spinel ferrites, the site preference of divalent and trivalent ions plays an important role in determining the electrical behavior of the ferrites. In this case, Cd^{2+} and Co^{2+} ions preferably occupy octahedral (B) sites, whereas Fe^{3+} distributed among both tetrahedral (A) and octahedral (B) sites. As the ionic radii of Ce^{3+} cations is larger as compared to Fe^{3+} ions, so it is more favourable that Ce^{3+} ions replace Fe^{3+} ions at B sites. Therefore, the increasing trend of dc electrical resistivity of samples with increase in Ce content (as shown in Fig. 8 (b)) is attributed to the reduced Fe^{3+} concentration at B sites.

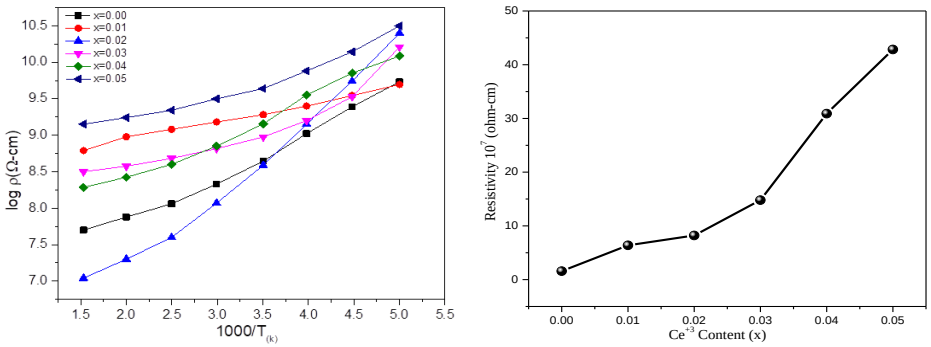

Fig. 8. (a) Plot (log ρ) resistivity versus 1000/T(K) at different Ce content (b) Variation of electrical resistivity versus Ce^{3+} content (x).

Furthermore, as cerium ions has large ionic radius which may cause to decrease the hopping rate of electron between Fe^{2+} and Fe^{3+} ions and consequently enhances the dc resistivity and activation energy. The electrical resistivity of the Ce^{3+} substituted Cd-Co nano ferrites was found in the range of 1.584×10^7 - 42.83×10^7 Ω-cm and is presented in Table 1. These values of electrical resistivity are in good agreement with the reported values in literature [28-29]. It is also observed that the resistivity of samples decreases with increase of temperature which confirms the semiconductor behavior of our samples. The activation energy (Ea) of charge carriers (electron and small polarons) is measured from the linear slope of the graph between log resistivity versus 1000/T by the following relation: $E_a = k_b$ x Slope where K_b is Boltzmann constant. The observed activation energy values are found in the range 0.02 - 0.05 eV and shows increasing trend with Ce content. The increasing trend of activation energy is attributed to the B site occupancy of Ce^{3+} cations. Similar results also have been reported by various researchers [30-31].

4. Conclusions

In this study, the effect of Ce^{3+} ions substitution in Cd-Co spinel ferrites is investigated. The samples were prepared by co-precipitation route. The prepared samples were sintered at 950 ^oC for 6 hours. The cations distribution of cerium substituted Cd-Co ferrites reliant on concentrations. The X-ray diffraction patterns show that all samples are single phase. The crystallite size was found in the range of 21.6 - 34.7 nm. The average lattice parameters were in the range of 8.47 - 8.67Å. The EDX spectra of Cerium substituted Cd-Co ferrites showed the characteristics peaks which ensured the presence of Cd, Fe, Co, Ce, and O. Current- Voltage characteristics shows that resistivity of materials decrease with increase of temperature due to the semiconductor behavior.

The calculated dc electrical resistivity value was in the range of 1.584×10^7 Ω-cm - 42.83×10^7Ω-cm. The resistivity of the synthesized material increases with the increase of Cerium substitution. The activation energy of the samples was in the range of 0.02 - 0.05 eV. In UV-Vis spectra, the observed peak indicates that nanocomposites are a photoactive compound and can be used in optoelectronic applications, magnetic recording media, security, switching and high frequency applications.

Acknowledgements

The author is thankful for providing characterization support to carry out this work under Govt. College University Faisalabad-RSP-Project # 159-PHY-5.

References

[1] S. Ramesh, et al., Cera. Inter., **40**(6), 8729 (2014).
[2] T. Shinde, A. Gadkari, P. Vasambekar, J. Magn. and Magn. Mate. **333,** 152 (2013).
[3] Z. Chen, et al., J. Alloy and Comp. **609**, 21 (2014).
[4] S. F. Wang, et al., J. Magn. and Magn. Mate. **365,** 119 (2014).
[5] I. Gul, A. Maqsood, J. of Alloy. and Comp. **465**(1), 227 (2008).
[6] D. R. Mane, D. D. Birajdar, S. Patil, S. E. Shirsath, R. H. Kadam, J. of Sol-Gel Science and Ttechnology **58**(1), 70 (2011).
[7] M. Hashim, S. Kumar, S. E. Shirsath, R. K. Kotnala, J. Shah, R. Kumar, Materials Chemistry and Physics **139**(2-3), 364 (2013).
[8] K. M. Batoo, S. Kumar, Inte. J. of Nanoparticles **2**(1-6), 416 (2009).
[9] R. Ahmad, I. H. Gul, M. Zarrar, H. Anwar, M. B. Khan Niazi, A. J. Khan, Magn. and Magn. Mate. **405**, 28 (2016).
[10] I. H. Gul, A. Maqsood, J. Alloy and Comp. **465**(1-2), 227 (2008).
[11] H. Z. Duan, F. L. Zhou, X. Cheng, G. H. Chen, Q. L. Li, J. Magn. and Magn. Mate. **424**, 467 (2017).
[12] N. Bahlawane, et al. Physical Chemistry Chemical Physics **11**(40), 9224 (2009).
[13] T. Abbas, M. A. Chaudhry, Materials Letters **53**(1-2), 30 (2002).
[14] J. Xie, et al., J. Magn. and Magn. Mate., **314**(1), 37 (2007).
[15] E. Rezlescu, et al., Crystal Research and Technology **31**(3), 343 (1996).
[16] M. I. Arshad, S. Ikram, K. Mahmood, A. Ali, M. A. Un Nabi, N. Amin, Y. Arooj, N. Sawaira, M. Asghar, M. Saleem, F. Jabeen, J. Batool, G. Mustafa, J. Ovonic Res. **14** (1), 27-34 (2018).
[17] M. A. Un Nabi, M. Sharif, G. Mustafa, A. Ali, K. Mahmood, N. Ali, N. Amin, M. R. Ahmad, N. Sabir, M. Asif, K. Hussain, M .S. Hasan, M. I. Arshad, Dig. J. Nanomater. Biostruct. **13** (4), 1111-1116 (2018).
[18] G. Mustafa et al., J. Magn. and Magn. Mate. **378**, 409 (2015).
[19] G. Mustafa et al., J. Magn. and Magn. Mate. **387**, 147 (2015).
[20] G. Mustafa, M. U. Islam, H. Anwar, M. Asif, M. I. Arshad, N. Sabar, M. R. Ahmad, G. Murtaza, M. A. Basharat, M. R. Saleem, J of Ovonic Research **14**(4), 261 (2018).
[21] K. P. Chae,Y. B. Lee, J. G. Lee, S. H. Lee,J.Magn. and Magn. Mate., **220**, 59 (2000).
[22] G. Mustafa, M. U. Islam, W. Zhang, Y. Jamil, A. W. Anwar, M. Hussain, M. Ahmad, J. Alloy and Comp. **618**, 428 (2015).
[23] A. Shitre, et al., Materials Letters **56**(3), 188 (2002).
[24] P. Kumar, S. K. Sharma, M. Knobel, M. Singh, J. Alloy and Comp. **508**, 115 (2010).
[25] N. Orhan, M. C. Baykul, J.Solid- State Electronics**78**, 147 (2012).
[26] P. Chand, A. Gaur, A. Kumar, J. Allo. And Compounds **539**, 174 (2012).
[27] O. M. Hemeda, M. M. Barakat, J. Magn. and Magn. Mate. **223**, 127 (2001).
[28] Hafiz Muhammad Tahir Farida, Ishtiaq Ahmad, K. A. Bhatti, Irshad Ali, Shahid M. Ramay, Asif Mahmood, Ceramics International **43**, 7253 (2017).
[29] E. Rezlescu, et al., Crystal Research and Technology **31**(3), 343 (1996).
[30] K. K. Bharathi, C. Ramana, J. of Mate. Research **26**(4), 584 (2011).
[31] E. Pervaiz, I. Gul, Inte. J. of Current Engg. & Technology **2**(4), 377 (2012).